Optimisation of Transmission Bandwidth for Indoor Cellular OWC System Using a Dynamic Handover Decision-Making Algorithm

D. Wu, Z. Ghassemlooy, H. Le Minh, S. Rajbhandari, and W. Lim*
Optical Communication Research Group, School of Computing, Engineering and Information Sciences, Northumbria University, Newcastle Upon Tyne, UK
E-mail: {dehao.wu, z.ghassemlooy, hoa.le-minh, sujan.rajbhandari}@northumbria.ac.uk
*Department of Engineering and Technology, University of Hertfordshire, Hatfield, AL10 9AB, UK

***Abstract*- In this paper, we propose a novel cellular optical wireless communications (COWC) system with four diffused cells. A dynamic handover scheme is proposed to make the link more flexible by the way of adaptive channel allocation in different environments. The simulation results show that the proposed algorithm offers almost five times of the maximum dynamic transmission bandwidth and energy efficiency compared to the worst scenarios when all base stations (BS)s are active .**

***Keywords*- Diffuse optical wireless communication, root mean square delay spread, and dynamic handover decision-making algorithm.**

I. INTRODUCTION

Indoor OWC has been widely studied since 1979 [1]. It provides a number of advantages; including a large and unlicensed bandwidth, a low cost and immunity to electromagnetic interference. With the increasing popularity of the high definition television and high data and video over the internet, the OWC technology becomes the complementary and viable solution for the bandwidth congestion currently experienced in the radio frequency multi-access networks [2]. Many research works on line of sight (LOS) and diffuse indoor OWC as well as visible light communications employing a wider divergence angle light emitting diode (LED) have been reported [3-6]. The LOS configuration offers the least path loss and maximum data throughput. Tracked LOS schemes employing a narrow beam transmitter offering high transmission data rate up to 30 Gb/s has been reported [7, 8]. However, this configuration has a limited coverage area, requires precise alignment or fast tracking mechanism and is susceptible to blocking and shadowing. The diffuse link offers excellent mobility and robustness to the blocking and shadowing in a close environment [9, 10]. However, diffuse links suffers from the multipath induced dispersion, which limits the maximum achievable data rates.

Multi-spot cellular configurations combine the benefits of both LOS and diffuse links [11-14]. In such systems mobile units (MU) could be in more than one cell but not necessarily all in active mode. Therefore it would be advantageous to switch off unused transmitters to save energy and resources. In this paper, a novel COWC system employing four diffused cells is proposed, where only cells with MUs are considered to be in the active mode. We propose a dynamic handover scheme whereby the transmission rate could be made adaptive for different environments, thus making the link more flexible as well as more energy efficient.

This paper is organised as follows: the system model is described in Section II. In Section III, the dynamic decision-making algorithm is presented. The multipath channel characteristics are detailed in Section IV. Then the simulation results and discussion are outlined in Section V. Finally, conclusions are drawn in section VI.

II. SYSTEM DESCRIPTION

The proposed indoor COWC system is shown in Fig. 1. The room has a dimension of 1.8×1.5×1 m^3 (length, width, height) which is divided into four equal sections. At the centre of each section, there is an optical BS composed of a transceiver module mounted on the ceiling. Each transmitter has a wide full width at half maximum (FWHM) divergence angle to provide a LOS link with minimum reflections within each cell, thus ensuring seamless high speed connectivity.

The MU is also composed of transceivers with the transmitter pointing upward the ceiling with a field of view (FOV) wide enough just to cover a single section on the ceiling. Employing circular cell shapes, there will be overlapping areas, where MU can have coverage by two BSs.

Here we are adopting circular cell shapes just to illustrate the concept, though any other shapes could also be used. there will be overlapping areas. The overlap between cells is necessary to ensure that communications is maintained during the handover time.

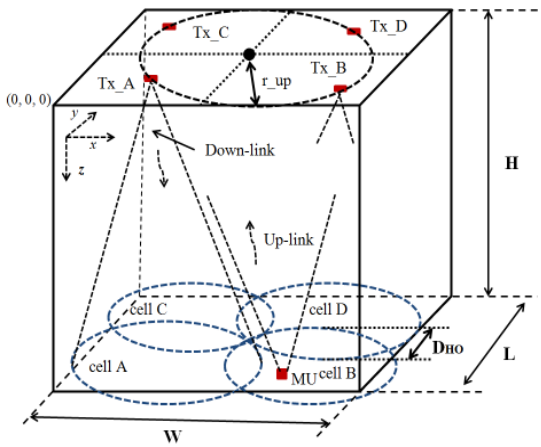

Fig. 1. Proposed 4- cell OWC systems for a typical indoor environment.

TABLE I
SPECIFICATION FOR INDOOR COWC SYSTEM

Room dimension (length, width, height)	1.8×1.5×1 m^3
Position of transmitter (Tx_A)	(0, 1.25, 1.25) m
Position of transmitter (Tx_B)	(0, 3.75, 1.25) m
Position of transmitter (Tx_C)	(0, 1.25, 3.75) m
Position of transmitter (Tx_D)	(0, 3.75, 3.75) m
LED output power	40 mW
LED field of view (FWHM) (down link)	80°
Beam radius r_up (up link)	1.7678 m
Photodectector active area	1cm^2
FOV of receiver	80°
Reflection coefficient of walls	0.8

By adopting a dynamic handover algorithm only the BS covering a cell where the MU is located is active and the rest are in the off mode. The handover time T_{ho} to ensure the seamless connectivity is given by:

$$T_{ho} < \frac{D_{HO}}{V}. \quad (1)$$

where D_{HO} is the horizontal overlap distance, and V is the typical speed of the MU. All the main parameters of the proposed system are specified in Table I.

III. THE DECISION-MAKING ALGORITHM

In the proposed indoor COWC system, 4-cell covers the entire room with each cell delivering the same data. The handover is initiated by detecting the uplink signal from the MU and the BS in each cell monitors presence of MU and request for data transmission. The flow chart for the handover process using the proposed decision-making algorithm for a single cell is shown in Fig.2. In state 1, the BS receiver is turned on to detect the presence of a MU within a cell. On detecting the MU, the BS will establish a link with MU for the data communication (see the state 2 in Fig.2). The duration between states 1 and 2 is equal to T_{ho}.

In real scenarios, MUs are randomly moving around within and between cells. To minimise the multipath interference and improve the energy efficiency, cells could be turned off when there are no active MUs within cells. This is carried out simply by checking the MU beacon signal as shown in states 2 and 3. If BS fails to an active MU within a cell, the corresponding BS is switched to the 'off-mode'. In real scenarios, MU located in overlapping area could be in communication with two BSs. To maximize the handover efficiency and to avoid too many handovers, the BS will continue to provide transmission for a short time in order to confirm the absence of MU. By double checking to see if there is no signal, BS will be switched to the 'off-mode' state, as illustrated by states 2 to 4 in Fig. 2.

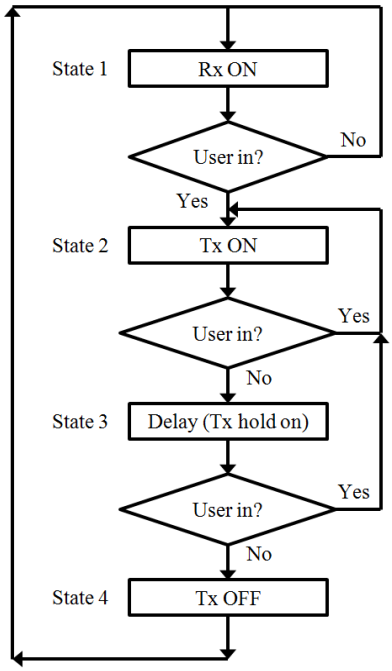

Fig. 2. Flow diagram for single cell decision-making algorithm

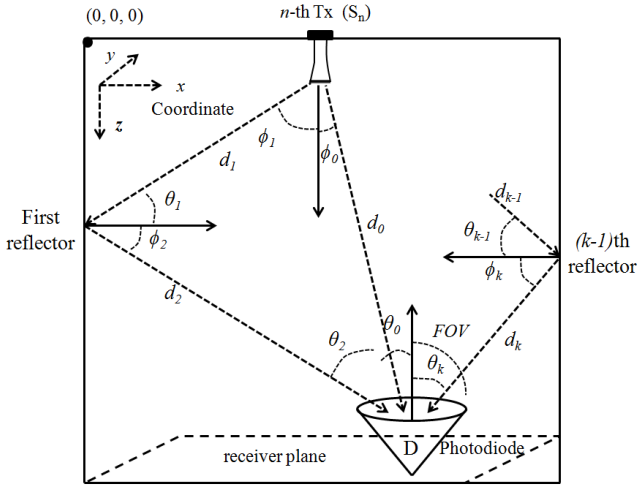

Fig.3. Geometry of source, detector and reflector

IV MULTIPATH CHANNEL CHARACTERISTICS

In the proposed 4-cell COWC system, both the path loss and multipath induced dispersion will limit the performance of the optical link. Fig. 3 shows the geometry of BS and MU, illustrating LOS and reflected paths. Depending on the position of the MU, the optical power after the first reflection cannot be neglected. The optical power distribution and the multipath dispersion at the MU plane can be characterized by the channel response $h(t)$. For typical optical communications system employing an LED as a transmitter, the radiation has a Lambertian pattern which given by [1]:

$$T(\emptyset) = \frac{m+1}{2\pi} cos^m(\emptyset), \quad (2)$$

where $m = -\ln(2)/\ln(\cos\varphi_{1/2})$ is the order of Lambertian radiant which is related to the transmitter semi-angle $\varphi_{1/2}$, (at half power). $\emptyset$ is the irradiance angle.

The LOS impulse response for a particular source S and a detector D (x, y, z), is given by [15]:

$$h^0(t; S, D) = \frac{T(\emptyset_0)}{{d_0}^2} A_R \cos\theta_0 \, \mathrm{rect}\left(\frac{\theta_0}{FOV}\right) \delta\left(t - \frac{d_0}{c}\right), \quad (3)$$

where A_R is the physical surface area of detector , θ_0 is the LOS incidence angle, FOV is the field of view of

detector, d_0 is the LOS distance between source *S* and receiver *D*, *t* is propagation time of ray and *c* is the speed of light. The rectangular function $\text{rect}(x)$ is given by:

$$\text{rect}(x) = \begin{cases} 1 & \text{for } |x| \leq 1, \\ 0 & \text{for } |x| > 1. \end{cases} \quad (4)$$

Assuming that all reflectors (i.e. plaster and acoustic-tiled walls, unvarnished wood) within the room are approximately Lambertian [1], the channel impulse response with multiple optical sources and multiple reflections is given by [15]:

$$h(t;\, S, D) = \sum_{n=1}^{N_{source}} \sum_{k=0}^{\infty} h_n^k(t;\, S, D). \quad (5)$$

The channel response for exactly *k* bounces with the extension for Lambertian pattern is given by [16]:

$$h^k(t;\, S, D) = \int_{\Psi} \left[\xi_0 \xi_1 \dots \xi_k \rho^k \, \text{rect}\left(\frac{\theta_k}{FOV}\right) \times \delta\left(t - \left(\frac{\sum_{k=0}^{\infty} d_k}{c}\right)\right) \right] dA_{ref} \;,\; k \geq 1 \quad (6)$$

where dA_{ref} is the small area of the reflecting element, ϕ_k and θ_k are the angles of irradiance and incidence, respectively, d_k is the distance from *k*-bounce to the detector (see Fig. 3)

$$\xi_0 = \frac{T(\phi_1)}{{d_1}^2} dA_{ref} \cos\theta_1 \;,\; \xi_1 = \frac{dA_{ref} \cos\phi_2 \cos\theta_2}{\pi d_2^2}$$

$$, \dots , \text{ and } \quad \xi_k = \frac{A_R \cos\phi_{k+1} \cos\theta_{k+1}}{\pi d_{k+1}^2}$$

The integration in (6) is performed with respect to the surface Ψ of all reflectors.

The severity of dispersion induced by a multipath propagation can be quantify using the root mean square (RMS) delay spread D_{rms}. The D_{rms} can be computed from the impulse response $h(t)$ using [11]:

$$D_{rms} = \left[\frac{\int (t-\mu)^2 h^2(t) dt}{\int h^2(t) dt} \right]^{\frac{1}{2}} \quad (7)$$

where the mean delay μ is given by:

$$\mu = \frac{\int t\, h^2(t) dt}{\int h^2(t) dt} \;. \quad (8)$$

V Results and Discussions

In order to carry out a comparative study of the different adaptive cases, the impulse response and the RMS delay spread is calculated using a computer simulation for a typical room. All the simulation parameters of the proposed COWC model are specified in Table I. Based on positions and numbers of MUs, there are four possible scenarios, which are outlined as follow:

Case A: MUs located within a single cell

If all MUs are located within a single cell, only the BS offering the coverage to cell can be in transmission mode and the remaining three BS are in 'off-mode'. Fig. 4 shows the simulated RMS delay spread distribution for this case. The near square area highlighted on the *x-y* axes is the location range for MUs. It illustrates that the maximum D_{rms} within the coverage area of active BS is ~ 0.2 ns, thus offering the maximum transmission rate of 500 Mbit/s as the maximum achievable data rate R_b without any equalization is $R_b \leq (10 D_{rms})^{-1}$[17]. For multiple MUs within a cell, the bandwidth can be shared using the multiple access control (MAC) technique as explained in [18].

Case B: Two adjacent BSs are active

If all MUs are located within two adjacent cells or in the overlapping areas between cells except centre of the room (see Fig. 1), two BSs are enabled to communicate with MUs. The simulated RMS delay spread for this case is depicted in Fig. 5. The maximum D_{rms} in this case is ~ 0.4 ns, which corresponds to almost half the maximum achievable data rate as in Case A.

Case C: Three BSs are active

Here 3 cells are active and one cell is in the 'off-mode' state. The simulated RMS delay spread is depicted in Fig. 6. The coverage area of the active BSs is also highlighted on *x-y* axes. The maximum RMS delay spread within coverage areas of active BSs is around ~1ns, which corresponds to the maximum achievable data rate of ~ 100 Mbit/s.

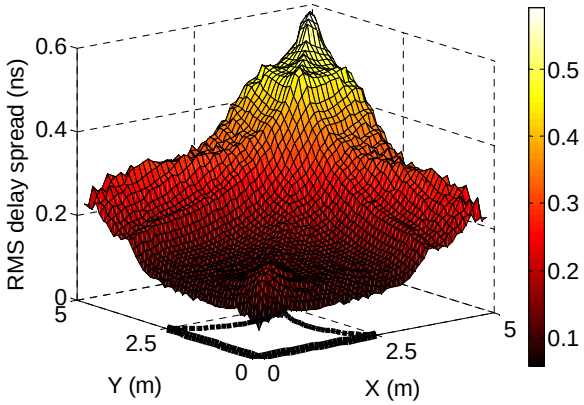

Fig. 4 Simulated RMS delay spread distribution within a typical room for a single active BS

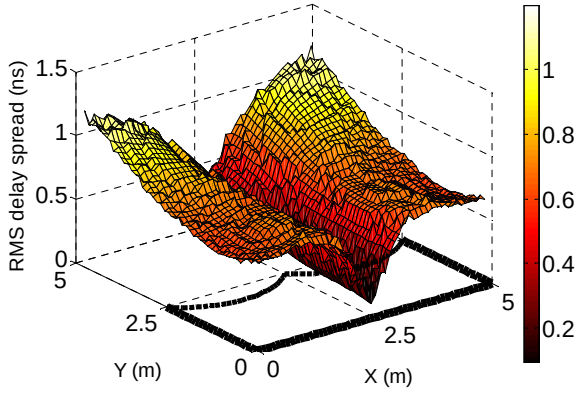

Fig. 5 Simulated RMS delay spread distribution within a typical room for two active BSs

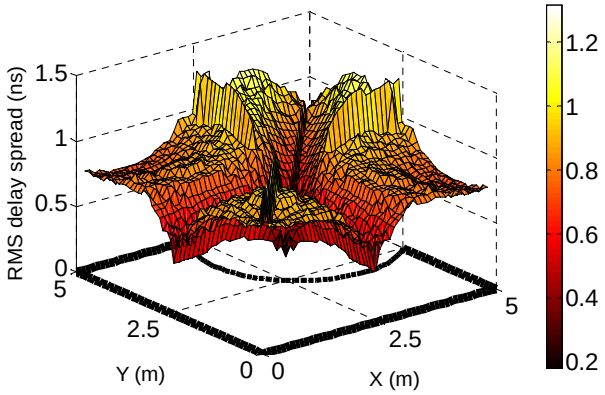

Fig. 6: Simulated RMS delay spread distribution within a typical room for three active BSs

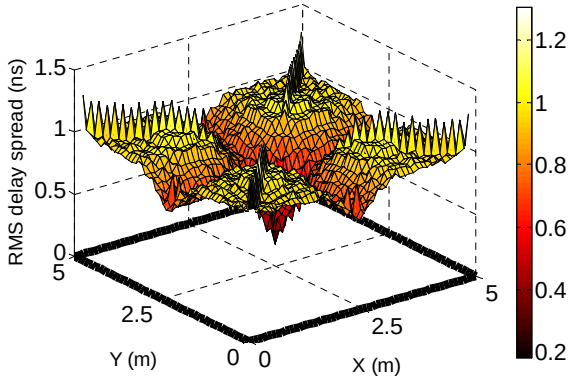

Fig. 7 Simulated RMS delay spread distribution within a typical room when all BSs are active.

Case D: When all BSs are active

This is the worth case, where the number of MUs within cells is high or MUs are moving around randomly within all four cells so that all BSs are in the active mode. The simulated RMS delay spread distribution for this case outlined in Fig. 7 Compared with the Cases A-C, the delay spread is the highest in this case with a maximum value of ~1.2 ns. Hence, the maximum achievable date rate is less than a fifth of the Case A. 500 Mbit/s of data rate can be delivered within a small coverage area with a radius of ~0.2 m.

It can be seen that as the number of active BSs increases, the RMS delay spread also increases due to higher multipath propagation and hence this would limit the maximum data rates. The problem can be overcome by using a cell with a small coverage area. However this will lead to an increase in number of transceivers and frequent handover, which in turn increases the overall system complexity. However, using a single cell to cover the entire room would result in high path loss and high delay spread. Therefore, optimization of the number of cells that could be employed is essential.

VI Conclusion

In this paper, we have modeled, and simulated a dynamic handover decision-making algorithm for the indoor COWC system. Based on locations of MUs and active BSs, the transmission capacity of the proposed system is analysed and optimised. The simulation results has shown that using an adoptive handover decision-making algorithm, the maximum transmission bandwidth for the best scenario can be improved more than five times comparing with the worst case.

Acknowledgment

The authors would like to acknowledge the support by EU Cost Actions of IC0802 and IC0110.

References

[1] F. R. Gfeller and U. Bapst, "Wireless in-house data communication via diffuse infrared radiation," *Proceedings of the IEEE*, vol. 67, pp. 1474- 1486, 1979.

[2] D. O'Brien, G. Parry, and P. Stavrinou, "Optical hotspots speed up wireless communication," *Nature Photonics*, vol. 1, pp. 245-247, 2007.

[3] Y. Tanaka, T. Komine, S. Haruyama, and M. Nakagawa, "A basic study of optical OFDM system for indoor visible communication utilizing plural white LEDs as lighting," *Proceeding of 8th International Symposium on Microwave and Optical Technology (ISMOT)*, pp. 303-306, 2001.

[4] D. O'brien, L. Zeng, H. Le-Minh, G. Faulkner, O. Bouchet, S. Randel, J. Walewski, J. A. R. Borges, K.-D. Langer, J. Grubor, K. Lee, and E. T. Won, "Visible light communication," in *Short-Range Wireless Communications: Emerging Technologies and Applications*, R. Kraemer and M. Katz, Eds.: Wiley Publishing, 2009.

[5] S. Rajbhandari, Z. Ghassemlooy, and M. Angelova, "Effective denoising and adaptive equalization of indoor optical wireless channel with artificial light using the discrete wavelet transform and artificial neural network," *IEEE/OSA Journal of Lightwave Technology*, vol. 27, pp. 4493-4500, 2009.

[6] R. J. Green, H. Joshi, M. D. Higgins, and M. S. Leeson, "Recent developments in indoor optical wireless systems," *IET Communications*, vol. 2, pp. 3-10, 2008.

[7] W. Ke, A. Nirmalathas, C. Lim, and E. Skafidas, "High-speed optical wireless communication system for indoor applications," *Photonics Technology Letters, IEEE*, vol. 23, pp. 519-521, 2011.

[8] H. Chen, H. van den Boom, E. Tangdiongga, and A. Koonen, "30Gbit/s Bi-directional Transparent Optical Transmission with an MMF Access and an Indoor Optical Wireless Link," *Photonics Technology Letters, IEEE*, vol. PP, pp. 1-1.

[9] J. M. Kahn and J. R. Barry, "Wireless infrared communications," *Proceedings of IEEE*, vol. 85, pp. 265-298, 1997.

[10] S. Jivkova and M. Kavehrad, "Shadowing and blockage in indoor optical wireless communications," in *Global Telecommunications Conference, 2003. GLOBECOM '03. IEEE*, 2003, pp. 3269-3273 vol.6.

[11] M. Kavehrad and S. Jivkova, "Indoor broadband optical wireless communications: optical subsystems designs and their impact on channel characteristics," *IEEE Wireless Communications*, vol. 10, pp. 30-35, 2003.

[12] S. Jivkova and M. Kavehard, "Multispot diffusing configuration for wireless infrared access," *IEEE Trans. Commun.,*, vol. 48, pp. 970-978, 2000.

[13] D. Wu, Z. Ghassemlooy, M. Hoa Le, S. Rajbhandari, and Y. S. Kavian, "Power distribution and q-factor analysis of diffuse cellular indoor visible light communication systems," in *European Conference on Networks and Optical Communications (NOC)*, Newcastle Upon Tyne UK, 2011.

[14] D. Wu, Z. Ghassemlooy, M. Hoa Le, and S. Rajbhandari, "Power distribution investigation of a diffused cellular indoor visible light communications system," in *PGNET2011*, Liverpool , UK, 2011.

[15] J. R. Barry, *Wireless Infrared Communications*. Boston: Kluwer Academic Publishers, 1994.

[16] L. Kwonhyung, P. Hyuncheol, and J. R. Barry, "Indoor channel characteristics for visible light communications," *IEEE Communications Letters*, vol. 15, pp. 217-219, 2011.

[17] T. S. Rappaport, *Wireless Communications*: Prentice-Hall, 2002.

[18] K. Woo-Chan, B. Chi-Sung, J. Soo-Yong, P. Sung-Yeop, and C. Dong-Ho, "Efficient resource allocation for rapid link recovery and visibility in visible-light local area networks," *Consumer Electronics, IEEE Transactions on*, vol. 56, pp. 524-531, 2010.